Published by :
http://www.ijert.org

International Journal of Engineering Research & Technology (IJERT)
ISSN: 2278-0181
Vol. 14 Issue 02, February-2025

Impact Ground Pressure Hazard Prediction for Deep Coal Mining Based on Multiple Feature Recognition and 2D Image Transformation

Weijiang Ma
Faculty of Transportation and Vehicle Engineering
Shandong University of Technology
ZiBo, China

Xiaowen Jiang
Faculty of Transportation and Vehicle Engineering
Shandong University of Technology
ZiBo, China

Jialin Zang
Faculty of Mechanical Engineering
Shandong University of Technology
ZiBo, China

lisha Wang
Faculty of Mathematics and Statistics
Shandong University of Technology
ZiBo, China

Mingwen Zheng
Faculty of Mathematics and Statistics
Shandong University of Technology
ZiBo, China

#Mingwen Zheng is Corresponding author

***Abstract*—Impact ground pressure poses a significant safety risk in the realm of deep coal mining. To preemptively detect and alert against these hazards, acoustic emission (AE) and electromagnetic radiation (EMR) signal monitoring are commonly employed. However, these signals often suffer from interference due to the mining environment and various other factors, which complicates the accurate execution of warnings. To address this challenge, we propose a novel prediction model. Initially, we extract the statistical characteristics of the coal mine sensor interference signals using mathematical statistics. Subsequently, we employ the Fourier transform to identify the frequency characteristics, and we analyze the periodicity of the signals using the ARIMA model. To further validate the effectiveness of our warning system, we convert the one-dimensional data into two-dimensional images. We then apply a combination of wavelet transform, Histogram of Oriented Gradients (HOG) feature extraction, and Support Vector Machine (SVM) classifier. Finally, we calculate the probability of successful warning using Long Short-Term Memory (LSTM) networks and percentage transformation methods. The amalgamation of these techniques is anticipated to enhance the precision and dependability of impact ground pressure early warnings, which is crucial for the safe operation of coal mines.**

***Keywords*—Statistical characteristics, Fourier transform, Autoregressive Integrated Moving Average model (ARIMA), two-dimensional image verification**

I. INTRODUCTION

Globally, coal has been one of the important resources supporting national energy and industry. In recent years, with the gradual increase in the depth of coal mining in China, the complexity of high geopathic stress in the deep part of coal mines has increased dramatically, and the intensity of impact ground pressure has been rising, with a significant increase in the risk, and the problem of impact ground pressure [1] has become a very important aspect of the safety of deep mines. Impact ground pressure is a violent dynamic phenomenon that occurs when the rock mass distributed around the shaft or working face is released due to the transient release of elastic deformation energy, which is extremely destructive and is a major disaster of global concern. Therefore, one of the urgent scientific and technological problems in the field of coal mine safety is how to monitor and warn impact ground pressure in time, as well as effectively prevent and control its occurrence. The aspects about coal mine safety have been widely studied, mainly entropy weighting and gray clustering [2, 3], fuzzy risk [4], data mining [5] and multi-intelligence body modeling [6]. However, in coal mining enterprises, risk early warning is often more important, and risk early warning can make a guarantee for the life safety of workers while reducing the loss of enterprises. Regarding coal mine risk early warning, a coal mining face safety early warning model was established based on FCM (fuzzy clustering model) and GA-BP (genetic algorithm-backpropagation neural network) [7]. Based on data mining, a gas outbreak and human factor risk warning model was established [8]. Using CNN-LSTM (Convolutional Neural Network-Long Short-Term Memory Neural Network) model [9] and IoT-supported sensors, a prediction model was constructed to improve the safety and productivity of underground coal mines [10].

Currently, impact ground pressure is monitored by various means, such as microseismic monitoring [11] and ground sound monitoring [12], in order to detect anomalies in time. In terms of prevention and control, measures such as reasonable arrangement of roadways, water injection into coal seams [13], and strengthening of support [14] are taken to reduce the possibility of impact ground pressure occurring and the degree

International Journal of Engineering Research & Technology (IJERT)
ISSN: 2278-0181
Vol. 14 Issue 02, February-2025

of harm. In order to reduce the impact of impact ground pressure on the mining industry, it is necessary to carry out the monitoring of impact ground pressure.

Accurate prediction of impact ground pressure is an important means to improve the safety of mining.Ju [15] studied the impact ground pressure early warning criterion with critical value and dynamic rate of change as indicators, and established a comprehensive multi-indicator impact ground pressure early warning method based on acoustic-electric and microseismic signals.Tian [16] determined a multi-parameter monitoring index system based on the analysis of microseismic, acoustic-electric, and stress precursor laws.Wang [17] selected important impact ground pressure danger characteristic factors and established GNSMA-SVM impact ground pressure danger level prediction model. The monitoring and warning of ground pressure in metal mines based on deep learning data analysis was proposed.Lukasz Wojtecki et al [18] predicted the risk of impact ground pressure hazard in active hard coal mines based on the principle that the prediction of impact ground pressure should require the assessment of the entire coal seam enclosure system, and used machine learning algorithms, such as neural networks, decision trees, random forests, gradient enhancement, and limiting gradient enhancement.

The research results of impact ground pressure monitoring indicators are increasingly abundant at home and abroad, different monitoring methods play a significant role in impact ground pressure monitoring and early warning, and the methods for establishing comprehensive evaluation models of impact ground pressure are increasingly diversified. However, the large amount of information provided by these methods makes it difficult to effectively integrate the multi-parametric indicators, and in the face of the challenge of dealing with the complex mining situation in the deep part of coal mines, it is necessary to establish a perfect impact ground pressure early warning system with the help of appropriate mathematical models.

To meet this challenge, this paper adopts multiple feature recognition and 2D image transformation techniques, and combines Fourier transform, ARIMA, wavelet transform, LSTM and other models by monitoring acoustic emission (AE) and electromagnetic radiation (EMR) signals in order to extract the feature signals and construct a scientific and accurate monitoring index and mathematical model. This model is applied to the deep mining environment of coal mines to predict the danger of impact ground pressure and calculate the correct prediction probability of the warning signal. The model not only effectively extracts the potential hazardous features before the occurrence of impact pressure, but also significantly improves the accuracy of impact hazard prediction. The scientific monitoring and early warning system of the model is conducive to safeguarding the life and property safety of coal mine workers and realizing the sustainable development of coal mine resources [19] [20]. The flow chart of the model is shown in Figure 1 below.

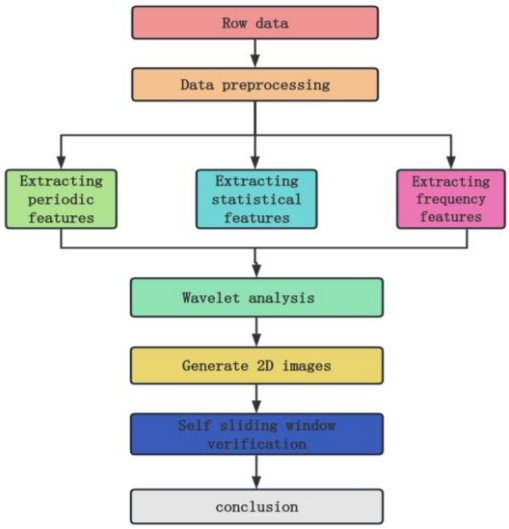

Figure 1 Model flow chart

Coal mine sensor signals are mainly divided into normal signal data, precursor signal data, interference signal data, sensor disconnection data and working face rest data.

II. MAIN JOB

1. Extraction and processing of interference signals

1.1 Extract the characteristics of the interference signal

In the coal mine early warning system, the interference signal and the precursor characteristic signal play a key role, so this paper will focus on these two types of signals.

Based on the existing data, we will analyze the interference signal in depth and extract its statistical characteristics. Specifically, we will calculate the mean, variance, standard deviation, maximum and minimum values of the jamming signal data in order to have a comprehensive understanding of the characteristics of the signals. The calculation formula is as follows:

$$\overline{X} = \frac{X_1+X_2+\cdots+X_n}{n} = \frac{\sum_{i=1}^{n} X_i}{n} \quad (1)$$

$$\sigma^2 = \frac{\sum_{i=1}^{n}(X_i-\bar{X})^2}{n} \quad (2)$$

$$\sigma = \sqrt{\frac{\sum_{i=1}^{n}(X_i-\overline{X})^2}{n}} \quad (3)$$

$$\max = Max\{X_1, X_2, \cdots, X_n\} \quad (4)$$

$$\min = Min\{X_1, X_2, \cdots, X_n\} \quad (5)$$

The results of the calculations are shown in Tables 1 and 2.

Table 1 EMR statistical characteristics

Mean value	Variance	Standard deviation	Maximum value	Minimum value
77.96	8229.37	90.72	500	0

Published by :
http://www.ijert.org

International Journal of Engineering Research & Technology (IJERT)
ISSN: 2278-0181
Vol. 14 Issue 02, February-2025

Table 2 AE statistical characteristics

Mean value	Variance	Standard deviation	Maximum value	Minimum value
59.97	6467.67	80.42	500	27

1.2 Fourier transform of the interference signal

$$X_k = \sum_{j=0}^{n-1} x_j \, e^{\frac{2\pi i}{n} kj} \quad (6)$$

$$x_j = \frac{1}{n} \sum_{k=0}^{n-1} X_k \, e^{-\frac{2\pi i}{n} jk} \quad (7)$$

Where X_k denotes the Fourier coefficients at frequency k, X_j is the value of the jth sample point in the time series, n is the total number of sampling points of the signal, and j is an imaginary unit. Through Fourier analysis, we can obtain the amplitude and phase information of the interference signal at different frequencies, which is of great significance for the accuracy and reliability of the warning system.

Then the data from Fourier transform [16] is plotted its frequency graph as shown in Fig. 2 and Fig. 3 below to observe the magnitude of its frequency. The frequency range is shown in Table 3.

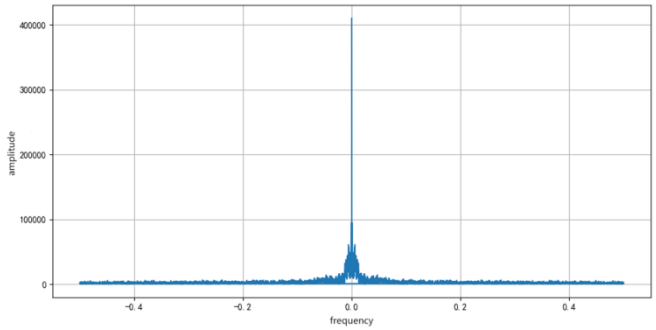

Fig. 2 Plot of EMR after Fourier transformation

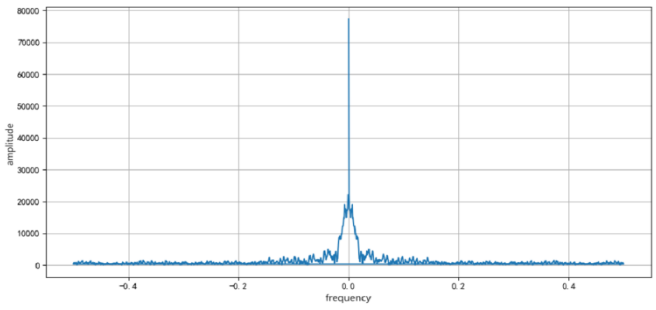

Fig. 3 AE graph after Fourier transform

Table 3 Frequency characteristics

form	EMR	AE
frequency range	±0.49971	±0.49108

1.3 Correlation analysis of interfering signals of acoustic emission (AE) and electromagnetic radiation (EMR) signals

Correlation analysis of the interfering signals of acoustic emission (AE) and electromagnetic radiation (EMR) signals is a crucial step in coal mine warning systems. The use of Pearson's correlation coefficient can help us to quantify the linear relationship between these two signals, thus revealing their interactions in the interference signal.

The Pearson [17] correlation coefficient is a statistical measure of the strength of the linear relationship between two variables and is calculated as follows:

$$r = \frac{\sum(X-\overline{X})(Y-\overline{Y})}{\sqrt{\sum(X-\overline{X})^2 \sum(Y-\overline{Y})^2}} = \frac{l_{XY}}{\sqrt{l_{XX} l_{YY}}} \quad (8)$$

l_{XX} denotes the sum of the squared deviations from the mean of X; l_{YY} denotes the sum of the squared deviations from the mean of Y; l_{XY} denotes the sum of the squared deviations from the mean of X and Y, The thermal matrix is shown below in Figures 4 and 5.

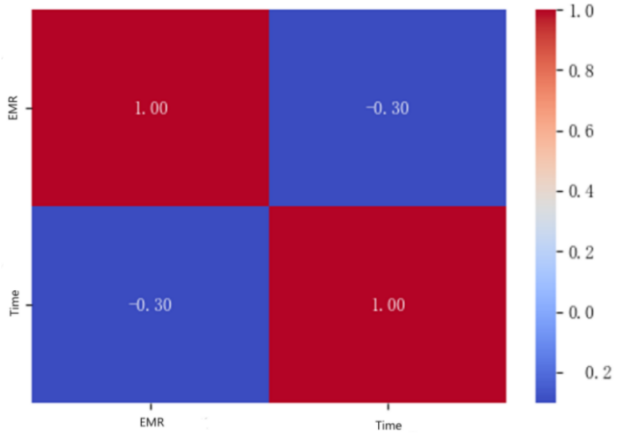

Fig. 4 Analytical results of Pearson correlation analysis of EMR with time

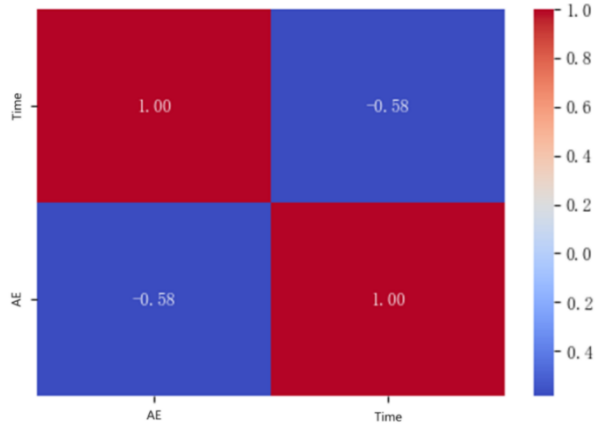

Fig. 4 Analytical results of Pearson correlation analysis of AE with time

The above figure shows the values of correlation coefficient s between EMR and AE and time respectively in the form of heat map, and the values are indicated by the color shades, according to the information in the figure, we can derive the following relationships: the correlation coefficient between EMR and time is -0.30, which is weakly negative correlatio n; the correlation coefficient between AE and time is -0.58, which is moderately negative correlation[18].

International Journal of Engineering Research & Technology (IJERT)
ISSN: 2278-0181
Vol. 14 Issue 02, February-2025

2. precursor feature signals

2.1 Extracting statistical features

Based on the existing precursor feature signal data, statistical features are extracted and the mean, variance, standard deviation, and standard error of the precursor feature signal data are calculated. As shown in Table 4 and Table 5 Below.

Table 4 EMR statistical characteristics

Mean	Variance	Standard Deviation	Standard Error
71.05	8445.58	91.90	0.82

Table 5 AE statistical characteristics

Mean	Variance	Standard Deviation	Standard Error
41.67	68.95	8.30	0.18

2.2 Extracting periodic features

The time series features are extracted using ARIMA [19] with the following formula.

ARIMA consists of the following two components: autoregressive model and moving average model and the formula is shown below.

$$y_t = \mu + \sum_{i=1}^{p} \gamma_i y_{t-i} + \epsilon_t + \sum_{i=1}^{q} \theta_i \epsilon_{t-i} \qquad (9)$$

The autoregressive part of the equation is shown below.

$$y_t = \mu + \sum_{i=1}^{p} \gamma_i y_{t-i} + \epsilon_t \qquad (10)$$

The moving average model formula is shown below.

$$y_t = \mu + \epsilon_t + \sum_{i=1}^{q} \theta_i \epsilon_{t-i} \qquad (11)$$

y_t is the current value. μ is a constant term, $p.q$ is an ordinal number (math.), γ_i is the autocorrelation coefficient, ϵ_t It's the error.

The preprocessed data is subjected to operations such as differencing and panning to make it conform to the smoothness and white noise requirements, and some of the results are shown in Fig. 6, Fig. 7, Fig. 8 , Fig. 9, Fig. 10 and Fig. 11 below.

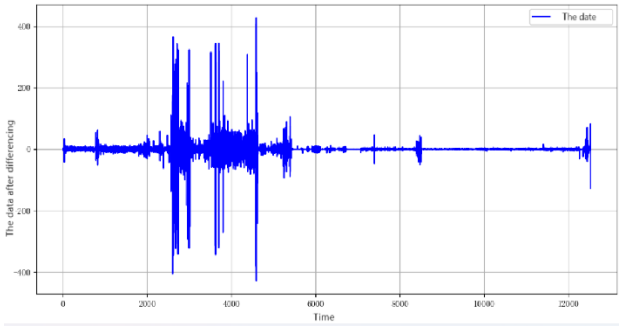

Fig. 6 Differential plot of EMR data

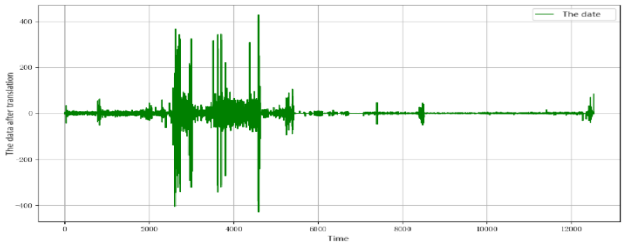

Figure 7 EMR data panning plot

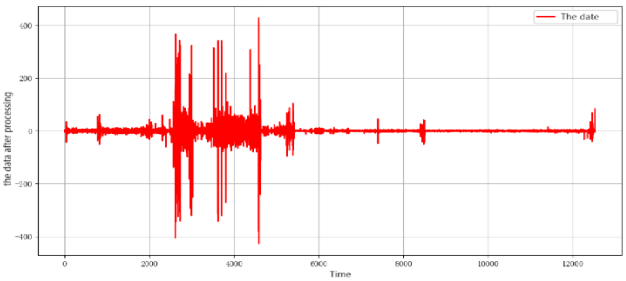

Fig. 8 White noise processing map of EMR data

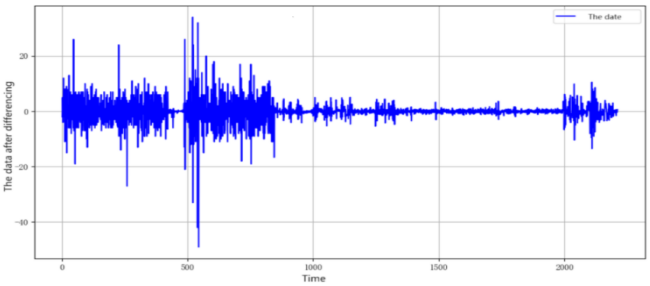

Fig. 9 Differential plot of AE data

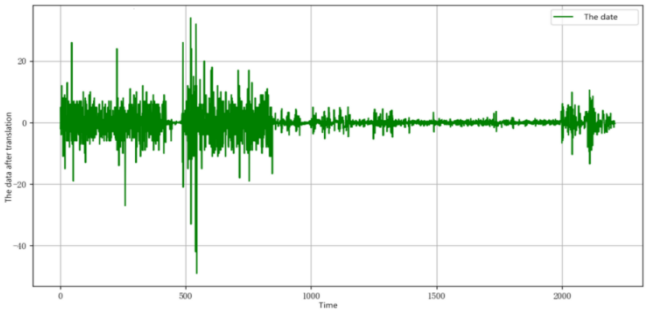

Figure 10 AE data panning plot

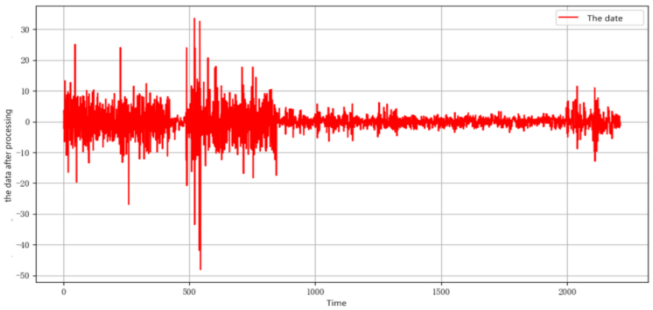

Fig. 11 White noise processing map of AE data

The program for ARIMA is written and for the processed data, the features are plotted as shown in Fig. 12 and Fig. 13 and the average features are shown in Table 6.

International Journal of Engineering Research & Technology (IJERT)
ISSN: 2278-0181
Vol. 14 Issue 02, February-2025

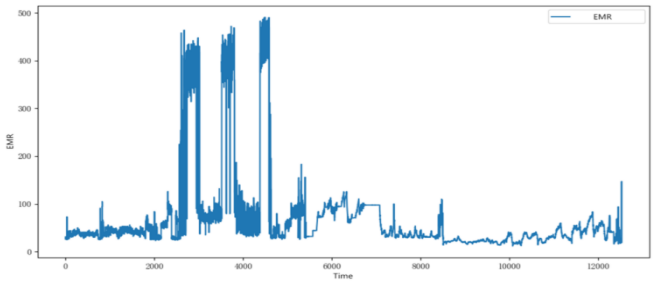

Fig. 12 EMR feature map extracted by ARIMA

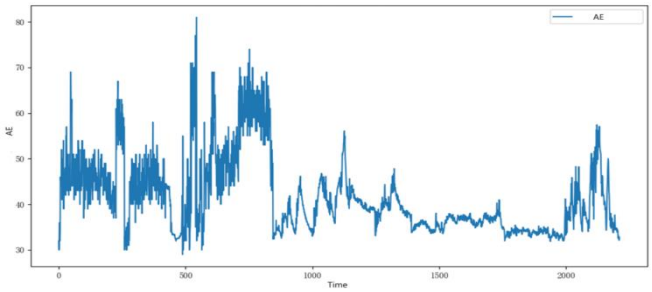

Fig. 13 ARIMA extracted AE feature map

Table 6 Average characteristics

form	EMR	AE
average characteristic	67.8651010	1.924774

3. 2D image conversion

3.1 Transformed 2D image using HOG for image feature extraction

Observing the dataset, the original one-dimensional data was considered to be converted into two-dimensional images for analysis and validation, considering that the precursor feature signals are less distinctive compared to the interference signals.

Continuous wavelet transform transforms the signal by using wavelet functions of different scales and positions to obtain local properties of the signal [20, 21].

$$W_x(a,b) = |a|^{-\frac{1}{2}} \int x(t)\hat{\psi}\left(\frac{t-b}{a}\right)dt \qquad (12)$$

$\psi(t)$ is the mother wavelet; $\psi(t)$ is the complex $\psi(t)$ conjugate; a is the scale parameter, $\psi(t)$ stretched when a>1 and $\psi(t)$ compressed when 0<a<1; b is the translation parameter; $|a|^{-1/2}$ is used to normalize the signal.

The specific steps are as follows:

step1: Select the wavelet function. First of all, we need to choose a suitable wavelet function as the base function of the transform. According to the signal data and the requirements of the question, the EMR data use "Complex Morlet" wavelet function, which is commonly used to analyze the spectral features, and the AE data use Mexican Hat wavelet function, which is commonly used for edge detection and feature extraction [22].

step2: The continuous wavelet transform involves the scale parameter a and translation parameter b, which need to be set in the appropriate scale parameter range. The scale parameter determines the frequency of the wavelet function, according to the data and conversion time, the scale parameter range is 1-127.

step3: Perform continuous wavelet transform. Conduct continuous wavelet transform with one-dimensional data and selected wavelet function to get a set of two-dimensional wavelet coefficients.

step4: Generate two-dimensional image. Use the obtained two-dimensional wavelet coefficients as pixel values to construct a two-dimensional image. The flow is shown in Figure 14. Select color

The color map is selected for image display, as shown in Figure 15 below.

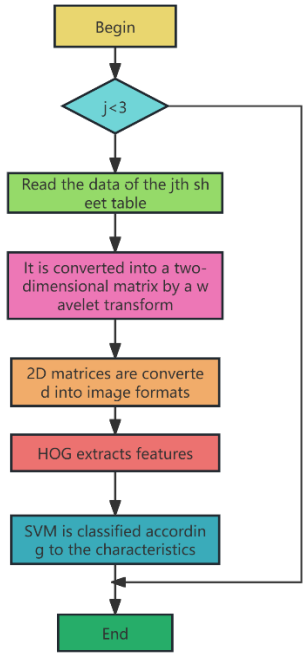

Fig. 14 Continuous wavelet flow chart

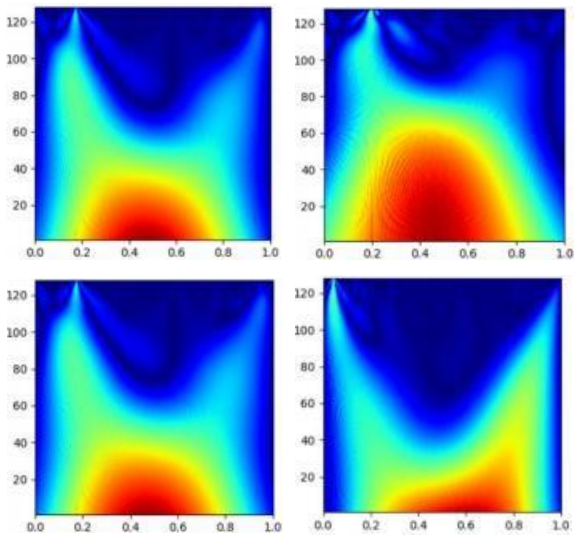

Fig. 15 Continuous wavelet transform diagram

International Journal of Engineering Research & Technology (IJERT)
ISSN: 2278-0181
Vol. 14 Issue 02, February-2025

The transformed 2D image is then subjected to image feature extraction using HOG. First the 2D matrix is converted into image format by normalize in open cv library [23]. After that feature extraction is done using HOG. Histogram of Oriented Gradient (HOG) feature is a feature descriptor used for object detection in computer vision and image processing. It consists of features by calculating and counting the histogram of gradients in a local region of an image [24].Hog features combined with SVM classifiers are widely used in image feature extraction and image recognition [25]. Finally SVM is utilized for feature matching, using SVM for classification, the classification objective is to find a hyperplane in the feature space, so that the distance from any sample point to the plane is greater than or equal to 1. If the sample is linearly indistinguishable, a kernel function is needed for nonlinear classification, that is, to obtain a nonlinear hyperplane, here nonlinear classification using linear kernel function [26, 27, 28].

$$K(x,z) = (\gamma x \bullet z + r)^{d} \qquad (13)$$

The results of the relevant parameters for SVM matching are shown in Table 7, where the first step of preprocessing is used to analyze the data continuity Processed data is analyzed with training set: validation set = 8:2.

Table 7 Results of relevant parameters

form	EMR-Accuracy	AE-Accuracy
numerical	0.739498	0.772727

The feature matching diagram is shown in Figure 18 below.

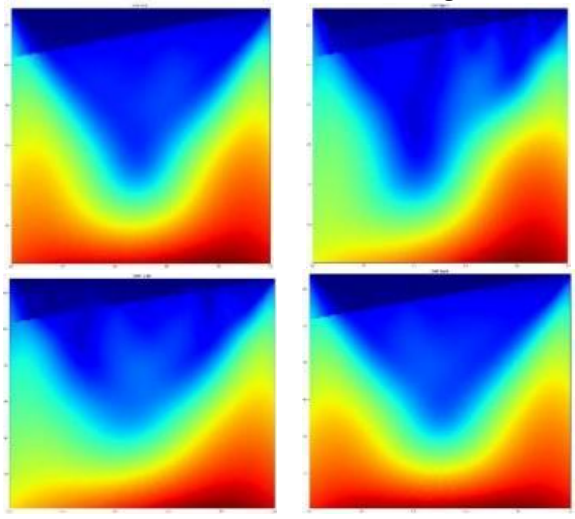

Fig. 18 Feature matching diagram

As can be seen from the figure, the precursor feature signal determined using the above model is consistent with the 2D image matching results. Afterwards, the signal features deter mined by the model are used to provide early warning for co al mine impact ground pressure.
For the data preprocessed by equal frequency sampling and l inear interpolation, the time sequence diagram is drawn to o bserve the change rule, as shown in Fig. 16 and Fig. 17 belo w.

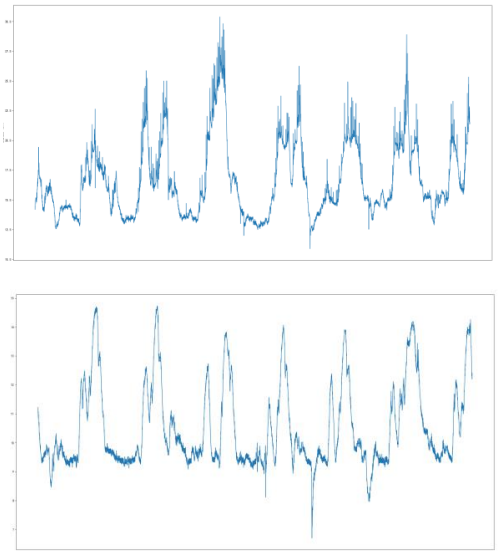

Figure 16 EMR Timing Diagram

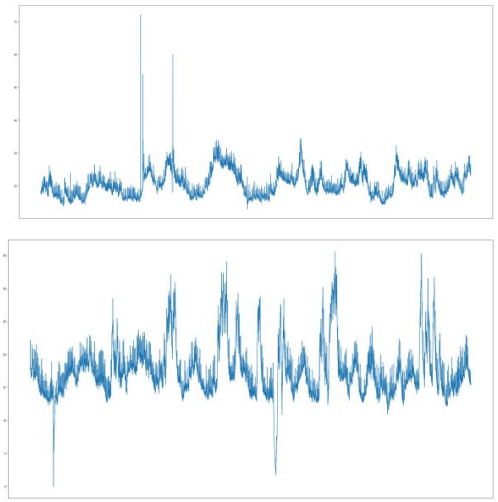

Figure 16 AE Timing Diagram

3.2 Building LSTM models for prediction
An LSTM model is built to predict it. An LSTM cell consist s of a memory cell C_t and three gate structures (input gate i_t, forget gate f_t, and output gate o_t) at time t, x_t represe nting the input data, h_t representing the hidden layer. X r epresents the vector outer product, and $+$ represents the su perposition operation. The formula is as follows:

International Journal of Engineering Research & Technology (IJERT)
ISSN: 2278-0181
Vol. 14 Issue 02, February-2025

$$
\begin{aligned}
f_t &= \sigma\left(U_f x_t + W_f h_{t-1} + b_f\right) \\
i_t &= \sigma(U_i x_t + W_i h_{t-1} + b_i) \\
u_t &= tanh(U_u x_t + W_u h_{t-1} + b_u) \\
c_t &= f_t * c_{t-1} + i_t * u_t \\
o_t &= \sigma(U_o x_t + W_o h_{t-1} + b_o) \\
h_t &= o_t * \tanh(c_t)
\end{aligned} \tag{14}
$$

U/W is the matrix weights, b represents the offset, σ is the sigm oid function [31], and the symbol * represents the vector outer pr oduct. The model diagram is shown in Figure 18.

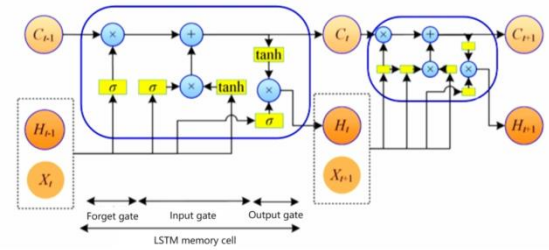

Fig. 18 LSTM model diagram

The value of percentage change is utilized to express the probability of its occurrence and the formula is shown below.

$$P_i = \frac{X - X_i}{X} \tag{15}$$

P_i denotes the probability of the occurrence of the ith event, X denotes the original feature, and xi (i varies from 1 to 20157) denotes the prediction result.

The dataset is then used for validation and the probability that the model can correctly warn is found as shown in Table 8 below.

Table 8 Probability of Early Warning

Early warning to EMR	72%
Early warning to AR	47%

III. CONCLUSION

Compared to existing methodologies, the majority of predictive techniques either involve analyzing a combination of multiple datasets, leading to predictions, or focus on a single type of data, such as geophones or imaging. The former approach is time-consuming due to the vast array of data types and the lengthy process of interaction and cooperation among them. It also suffers from low fault tolerance and incurs substantial labor and instrumentation costs due to the collection of various data types. In contrast, the latter method, which analyzes a single data type, offers higher accuracy but is limited in scope. This thesis presents a method that can be applied to most mining areas without being constrained by actual mining conditions, and it effectively explains the degree of correlation between predictions and real-world outcomes. Regarding prediction accuracy, many papers merely provide an approximate law of characteristics without a clear definition. In contrast, this thesis derives formulas for these characteristics, supported by clear data or images, resulting in higher accuracy. In summary, the method employed in this thesis offers significant advantages over traditional predictive methods in terms of accuracy, cost, and prediction time. It enables the most accurate predictions to be made in the shortest possible time, greatly enhancing the safety of people and property in mining areas.

ACKNOWLEDGMENT

Acknowledgements. This work is funded by the Natural Science Foundation of Shandong Province (Grant Nos.ZR2023MF036), the National Natural Science Foundation of China (Grant Nos. 12172201).

Declaration of competing interest

The authors declare that they have no known competing financial interests or personal relationships that could have appeared to influence the work reported in this paper.

REFERENCES

[1] DU Linming, TIAN Xinyuan, CAO Anye, et al. Current situation and problems of impact ground pressure prevention and control in coal mines in China[J]. Journal of Coal,2022,47(01):152-171.DOI:10.13225/j.cnki.jccs.yg21.1873.

[2] X.H.; Zhang, D.H. Prediction of maritime logistics service risks applying soft set based association rule: An early warning model. reliab. eng. syst. Saf. 2021, 207, 107339. [CrossRef]

[3] Jing, S.F.; Liu, X.W.; Gong, X.Y.; Tang, Y.; Xiong, G.; Liu, S.; Xiang, S.G.; Bi, R.S. Correlation analysis and text classification of chemical accident cases based on word embedding. Process Saf. Environ. Prot. 2022, 158, 698-710.[CrossRef]

[4] Jiskani, I.M.; Han, S.; Rehman, A.U.; Shahani, N.M.; Tariq, M.; Brohi, M.A. An Integrated Entropy Weight and Grey Clustering Method-Based Evaluation to Improve Safety in Mines. Min. Metall. Explor. 2021, 38, 1773-1787.[CrossRef]

[5] Jiskani, I.M.; Yasli, F.; Hosseini, S.; Rehman, A.U.; Uddin, S. Improved Z-number based fuzzy fault tree approach to analyze health and safety risks in surface mines. resour. policy 2022, 76, 102591. [CrossRef]

[6] Jo, B.W.; Khan, R.M.A. An Event Reporting and Early-Warning Safety System Based on the Internet of Things for Underground Coal Mines: a Case Study. Appl. Sci. 2017, 7, 925.[CrossRef]

[7] Tang, Q.L.; Lei, M.F.; Zhu, B.B.; Peng, L.M.; Wu, W.M.; Shi, C.H. Design and Application of Risk Early Warning System for Subway Station Construction Based on Building Information Modeling Real-Time Model. Adv. Civ. Eng. 2021, 2021, 8898893. [CrossRef]

[8] Teng, Y.; Sun, Y.; Yang, H.H.; Guo, X.Y.; Chen, X.L. Research on the relationship between enterprise safety production management mode and employees' safety behavior based on social cognition. ' safety behavior based on social cognition and behavior incentive theory. Int. J. Occup. Saf. Ergon. 2022, 2021, 2022957. [CrossRef] [PubMed]

[8] Wang, Q.Q.; Cheng, C.; Zhang, C.; Zhang, J.H.; Ning, K.Y. Fuel Gas Enterprise Accident Risk Assessment Based on BP Neural Network. in Man-Machine- Environment System Engineering (Mmese 2019); Lecture Notes in Electrical Engineering; Springer: Singapore, 2020; Volume 576, pp. 759- 767.

[9] Yuan Luo, YongChao Zeng, RunZhe Lv, and WenHao Wang, "Dual-stream VO: Visual Odometry Based on LSTM Dual-Stream Convolutional Neural Network", Engineering Express, vol. 30, no. 3, pp926-934,2022

[10] Pan Junfeng,Liu Shaohong,Ma Wentao,et al. The occurrence law and classification and prevention of impact ground pressure in Shaanxi coal mine [J]. Coal Science and Technology, 2024, 52 (01): 95-105.

[11] PAN Liyou, SHI Mingwei, DONG Wenzhuo, et al. Prevention and control of impact ground pressure in overlying coal pillar area based on composite weakened structure [J]. Mining Safety and Environmental Protection, 2023, 50 (05): 99-104+110. DOI:10.19835/j.issn.1008-4495.2023.05.016.

[12] Lai M, Zhao W-W, Zhang L, et al. Analysis and optimization of the effectiveness of impact hazard monitoring and warning in deep high-stress working face [J]. Coal Science and Technology, 2023, 44 (05): 91-98. DOI:10.19896/j.cnki.mtkj.2023.05.017.

[13] Cao H-T. Analysis and prevention of impact hazards in the outer fault zone of a thick coal seam working face [J]. Coal Science and Technology, 2023, 44 (05): 121-126. DOI:10.19896/j.cnki.mtkj.2023.05.022.

[14] Yu Y. Research on the stress evolution law and prevention technology during the cross-passing of cross-layer roadway in deep impact area [J]. Coal Science and Technology, 2023, 44 (05): 161-165+169. DOI: 10.19896/j.cnki.mtkj.2023.05.030.

[15] JU Yunqiang. Research on the precursor characteristics and early warning method of impact ground pressure in the Tiger Terrace coal mine [D]. China University of Mining and Technology,2020.DOI:10.27623/d.cnki.gzkyu.2020.000351.

International Journal of Engineering Research & Technology (IJERT)
ISSN: 2278-0181
Vol. 14 Issue 02, February-2025

[16] Tian Jiawei. Research on the fusion of multi-source information of im pact ground pressure early warning in Hengda coal mine[D]. China U niversity of Mining and Technology, 2023.DOI:10.27623/d.cnki.gzky u.2023.001977.
[17] Wang Shanyu. Characterization of coal mine impact ground pressure danger and intelligent prediction and warning research[D]. Anhui Uni versity of Technology, 2023.DOI:10.26918/d.cnki.ghngc.2023.00042 2.
[18] Wojtecki L, Iwaszenko S, Apel D B, et al. Use of machine learning al gorithms to assess the state of rockburst hazard in underground coal m ine openings [J]. Journal of Rock Mechanics and Geotechnical Engin eering:English Edition, 2022, 14(3):703-713.
[19] Gong Shuang,Shen Wenlong,Nan Hua. Exploration on the constructio n of case teaching system of graduate course "Mine Power Hazard" [J]. Education and Teaching Forum, 2023, (43): 105-108.
[20] Information [J]. China Coal Industry, 2023, (10): 39-41.
[21] JIANG Sheng,WU Jinmin,LU Mingfeng,et al. Wavelength measurem ent by Michelson interferometry based on fractional Fourier domain si gnal processing [J]. Journal of Metrology, 2023, 44 (11): 1652-1658.
[22] YUAN-SHANG ZHAO, WEI-FANG LIN. Study of typical scenarios based on Pearson's correlation coefficient fusion of peak density and e ntropy weight method [J]. China Electric Power, 2023, 56 (05): 193-2 02.
[23] Cheng Juanjuan. An empirical study on the relationship between resea rch and teaching in colleges and universities--an analysis based on Pea rson's correlation coefficient [J]. China University Science and Techn ology, 2022, (10): 46-52. DOI:10.16209/j.cnki.cust.2022.10.016.
[24] Moret G R ,Martí C A ,Fernández A I , et al. Inflammatory biomarker s and psychological variables to assess quality of life in patients with i nflammatory bowel disease: a cross-sectional study. [J]. Annals of me dicine, 2024, 56 (1): 2357738-2357738.
[25] HE Haibo, WU Huilin, XU Bo. A prediction method of GNSS pseudo range observations based on ARIMA model [J]. Surveying and Mappi ng Standardization, 2023, 39 (02): 21-25. DOI:10.20007/j.cnki.61-127 5/P.2023.02.05.
[26] Q. Liu. Analysis of coal mining machine operation state prediction ba sed on the combination of Arima model and BP neural network [J]. Sh anxi Coking Coal Science and Technology, 2023, 47 (05): 23-27.
[27] An Yitong. Research on three-dimensional shape recovery method of workpiece based on two-dimensional image [D]. Dalian University of Technology, 2022. DOI:10.26991/d.cnki.gdllu.2022.001343.
[28] Zhang T. Research on unsupervised 3D model retrieval method based on 2D images [D]. Tianjin University, 2021. DOI:10.27356/d.cnki.gtj du.2021.005341.
[29] Sun Yunhan. Depth estimation of 2D images based on deep learning [D]. Jiangsu University of Science and Technology, 2020. doi:10.271 71/d.cnki.ghdcc.2020.000347.
[30] Flores G I F ,Klünder K M ,Teros L T M , et al. Development and Val idation of a Method of Body Volume and Fat Mass Estimation Using Three-Dimensional Image Processing with a Mexican Sample.[J]. Nut rients, 2024, 16 (3).
[31] Dongfang. Square wave continuous wavelet transform based on MAT LAB [J]. Light Industry Science and Technology, 2014, 30 (05): 60-6 1.
[32] GANG Gang, WANG Yunsheng, HE Xianlong, et al. Characterizatio n of slope dynamic response based on continuous wavelet transform-- An example of the M_s6.0 magnitude earthquake in Changning, Sichu an [J]. Chinese Journal of Geological Hazards and Prevention, 2021, 3 2 (02): 1-8. DOI:10.16031/j.cnki.issn.1003-8035.2021.02.01.
[33] An Bashou, Wang Xuemei, Huang Xiaoyu, et al. Hyperspectral estim ation of heavy metal cadmium in soil based on continuous wavelet tra nsform [J]. Earth and Environment, 2023, 51 (02): 246-253. DOI:10.1 4050/j.cnki.1672-9250.2022.50.044
[34] Cheng L, Lu JG. Feature extraction of welding seam image of mining equipment based on deep learning [J]. Coal Mine Machinery, 2024, 4 5 (05): 176-178. DOI:10.13436/j.mkjx.202405054.
[35] Fei M ,Shen Z ,Song Z , et al. Distillation of multi-class cervical lesio n cell detection via synthesis-aided pre-training and patch-level featur e alignment [J]. Neural Networks, 2024, 178 106405-.
[36] Zeng Yi, Wu Jiamin, Bian Yuewei, et al. Prediction of large-diameter mud-water balanced shield tunneling attitude based on LSTM algorith m [J/OL]. Tunnel Construction (in Chinese and English), 1-11[2024-0 6-07].